

Wettability and interfacial reaction of alumina and zirconia by reactive silver–indium base alloy at mid-temperatures

X. M. XUE, J. T. WANG

State Key Laboratory of RSA, Institute of Metal Research, Academia Sinica, Shenyang 110015, People's Republic of China

Z. T. SUI

Department of Non-ferrous metals, Northeast University of Technology, Shenyang 110006, People's Republic of China

The wettability of sintered alumina and sintered zirconia by silver–indium base alloy with small titanium additions (< 5 at %) has been investigated using sessile drop tests conducted in a vacuum of 1.1–2.0 mPa at mid-temperatures 873–1150 K. The addition of titanium can effectively induce the silver–indium base alloy to wet the alumina and zirconia. Under the present experimental conditions, the silver–indium–titanium alloys on the alumina exhibited excellent wettability characterized by a minimum titanium addition for wetting transition (contact angle $< 90^\circ$) of less than 0.2 at % Ti, whereas the alloy on the zirconia exhibited the minimum around 0.5 at % Ti. The minimum contact angle of the alloy–alumina system is about 5° and that of the alloy–zirconia system is about 15° . X-ray diffraction analysis shows that the reaction phases formed in the interface of the silver–indium–titanium alloy on the alumina are TiO_2 , TiO and Ti_2O , and those formed in the interface of the alloy on the zirconia are TiO and Ti_2O .

1. Introduction

With the advance in ceramics and the increasing use of ceramic materials, metal–ceramic joining and the production of composites have received considerable attention. Among the various joining processes, brazing is expected to emerge as an important technique. The most important step in using this technique for a metal–ceramic joint is the design of the filler metal.

The key problem in designing filler metals for brazing and soldering of ceramic and metals is of the interfacial bonding between ceramic and filler metal, and an important area in studying the interfacial bonding is the wettability of the ceramic by the filler metal with its effective factors. Hence, much work has been done in this area [1–15].

Oxide ceramics, especially alumina and zirconia, have been used extensively in various fields. There have been many reports on the wettability of alumina and zirconia by liquid metals [6–15]. In these reports the wetting characteristics of the ceramics by liquid metals were investigated at high temperatures over 1173 K, apart from that by tin base alloys, and thus brazing would be carried out at higher temperatures.

There are several ceramic components where the service temperature of the ceramic–metal joint is lower than 773 K. For such components, it is preferable to use a lower brazing temperature, and hence it is necessary to design the filler-metal brazing at mid-

temperatures: 773–1173 K. Although tin–titanium alloy could wet alumina at mid-temperatures [7], its solidus temperature was very low, therefore the utilization of the alloy as a filler would be restricted.

The silver–indium system alloy is an important series of brazing material mainly used in the electronics industry. In this paper, $\text{Ag}_{65}\text{In}_{35}$ base alloy with a small titanium (< 5 at %) addition was investigated in the 873–1173 K temperature range; the solidus temperature of the Ag–In base alloys is 873 K and its liquidus temperature lies between 900 K and 925 K. Qualitative analysis of the experimental results was made using reaction thermodynamics.

2. Experimental procedure

2.1. Materials

The metals used in this work were silver, indium and titanium. Of the metals used, silver and indium were of over 99.999% purity, titanium was of over 99.99% purity. For the alloy samples used in the experiment, the atomic ratio of Ag:In was a constant value, i.e. $X_{\text{Ag}}:X_{\text{In}} = 65:35$. The composition of the various alloy samples is listed in Table I.

The various alloys identified in Table I were produced *in situ* by machining a disc of silver, 3 mm diameter and about 1 mm thick, on which the required amount of alloying element and of middle alloy

TABLE I Nominal alloy composition (at %). $X_{Ag}/X_{In} = 65/35$

Ag-In base alloy with Ti	Substrate
AgIn-0.065Ti	Al ₂ O ₃
AgIn-0.20Ti	
AgIn-0.47Ti	
AgIn-1.10Ti	
AgIn-2.20Ti	
AgIn-4.90Ti	ZrO ₂
AgIn-0.20Ti	
AgIn-0.50Ti	
AgIn-1.00Ti	
AgIn-2.80Ti	
AgIn-4.70Ti	

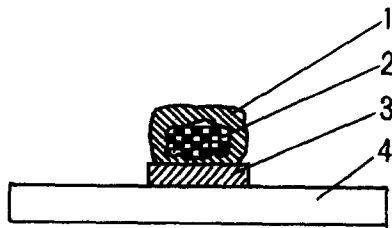


Figure 1 In situ test of an alloy sample with (1) pure indium, (2) Ag-In-Ti middle alloy, (3) pure silver, and (4) oxide substrates.

were placed as in Fig. 1, the total weight of the sample being 0.1–0.125 g. The AgIn-Ti middle alloy (10 at % Ti) was prepared by arc-melting the constituent metals under a vacuum atmosphere of about 2.0 mPa, the weight of the middle alloy nugget being 5.0 g. The weight loss on melting was less than 1% for the alloy. Electron probe microanalysis (EPMA) of the nugget showed that the composition of the middle alloy was very even. Some pieces of the middle alloy nugget were used to produce the alloy samples listed in Table I as shown in Fig. 1.

The ceramic substrates used in this work were hot-pressed sintered alumina and zirconia, 15 mm diameter and 2 mm thick. The surface of the substrates was polished with SiC powder and 0.5 μm diamond, and then cleaned with nitric acid. Finally it was heated to 1273 K in air, for a holding time of 20 min prior to use. The chemical composition of the alumina substrate was 99.0% Al₂O₃, 0.4% MgO, 0.6% SiO₂, and of the zirconia substrate was 96.8% ZrO₂, 2.2% Y₂O₃, 1.0% Al₂O₃.

2.2. Apparatus and methods

The sessile drop method was employed to measure the contact angle between molten alloys and the ceramic substrates at the mid-temperatures. The apparatus for measurement consisted of two groups as shown in Fig. 2, i.e. the furnace and the measuring television and microcomputer processing system. The furnace part was quite similar to that in earlier reports [16, 17], and the measuring system principle was as follows: first, the video frequency signal of the camera is amplified and clipped, and then the specific feature

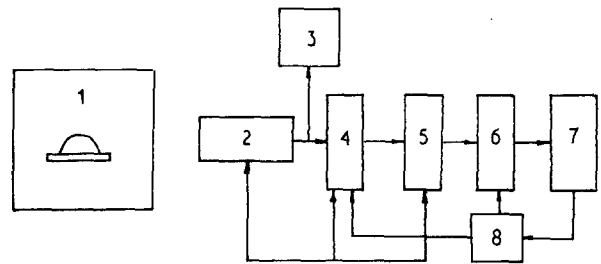


Figure 2 Principles of the apparatus used for measurement of the surface tension of the liquid metal and the contact angle on the solid substrate. 1, furnace; 2, black and white camera; 3, picture monitor; 4, specific feature signal separator and digital window; 5, data acquisition card; 6, interface; 7, microcomputer; 8, sync-signal allotter.

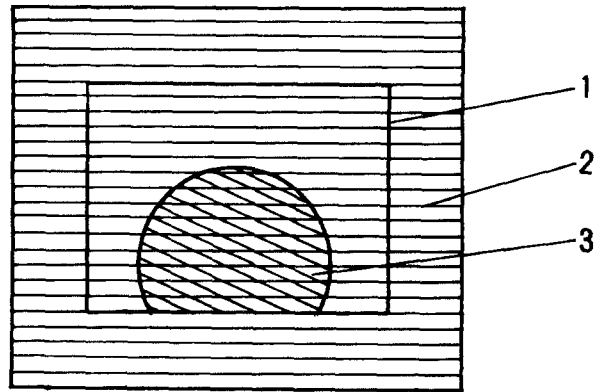


Figure 3 Picture monitor: 1, digital window; 2, scanning line; 3, test sample picture.

signals, which are representative of geometrical parameters of the test sample, are separated by control of the digital window, as shown in Fig. 3.

In Fig. 3, only the picture signals in the digital window can pass through the specific feature circuit. The signals are features which are only representative of geometrical parameters of the test sample after time synchronous signals and background signals of the window are filtered out. Then the signals are collected on a data-in acquisition card, where they are sampled and undergo analogue-to-digital conversion. After data sampling, the surface tension and density of the liquid alloy and the contact angle between the molten alloy and substrate can be calculated by CPU using the data and calculus.

Both ceramic substrates and metal samples were cleaned by ultrasonic vibration in acetone for 20 min before the experiments. The ceramic substrate then was placed in the furnace, its upper surface levelled carefully, and the alloy sample positioned on it as in Fig. 1 before the furnace was closed. After the system was evacuated down to a pressure of 2.0 mPa, the samples were heated at 5 K min⁻¹ to 700 K, and held there to outgas for 90 min. The samples were then heated at the same rate to 850 K, then to other temperatures at 50 K intervals and held at each temperature for 30 min to establish an equilibrium contact angle between the molten alloy and the ceramic substrate. The vacuum in the chamber during the test was held at 1.1–2.0 mPa. To keep the atmosphere

around the samples as clean as possible, Zr-10RE alloy filings (RE: rare-earth, (~wt %) 50Ce, 25La, 16Nd, 6.0Pr) were placed in the chamber and around the substrate.

3. Results and discussion

3.1. Wettability of alumina and zirconia by molten $\text{Ag}_{65}\text{In}_{35}$ alloy

In order to study the effect of reactive elemental additions on the wettability between the alloy and the ceramic substrates, the wetting of $\text{Ag}_{65}\text{In}_{35}$ alloy on both oxides was investigated. The contact angles between the $\text{Ag}_{65}\text{In}_{35}$ alloy melt and Al_2O_3 and ZrO_2 at various temperatures are shown in Fig. 4. It is obvious from this figure that the contact angles of the molten Ag-In alloy on Al_2O_3 and ZrO_2 show values higher than 140° in the test-temperature range. No clear temperature dependence of contact angle can be observed in the molten Ag-In alloy/ Al_2O_3 and Ag-In/ ZrO_2 systems. After the experiments, the solidified droplet of Ag-In alloy was completely separated from the substrate, thus indicating that there is no chemical adhesion force between the molten alloy and the ceramic substrates in this temperature range, i.e. no chemical reaction took place in the interface of the molten Ag-In alloy on both oxides, and only physical adhesion existed between them.

The contact angle between the molten Ag-In alloy and ZrO_2 was higher than that between the molten Ag-In alloy and Al_2O_3 at various test temperatures; the difference was about 3° – 10° . This may be caused mainly by a difference in the solid surface energy of both oxides. The calculated values of the solid surface energy of the oxides are: Al_2O_3 , $\gamma_s = 905 \text{ mJ m}^{-2}$ [18]; ZrO_2 , $\gamma_s = 800 \text{ mJ m}^{-2}$ [18]; thus the surface energy of Al_2O_3 is higher than that of ZrO_2 .

3.2. Wettability of AgIn-Ti/ ZrO_2 system

The temperature dependence of the contact angle between the Ag-In base alloy with titanium addition and a ZrO_2 substrate is shown in Fig. 5a. From this figure it can be seen that a small titanium addition to the Ag-In base alloy significantly promotes the wetting of ZrO_2 by the molten alloy, and the contact angle of the system is lowered with increasing temper-

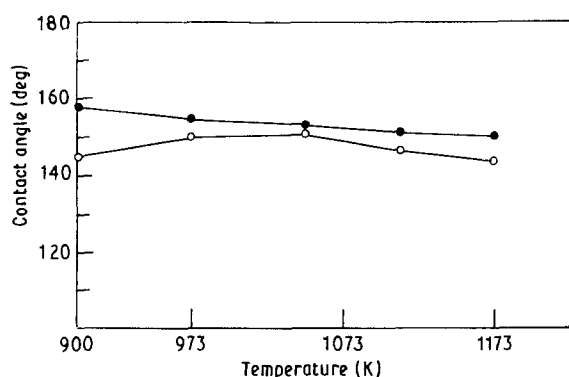
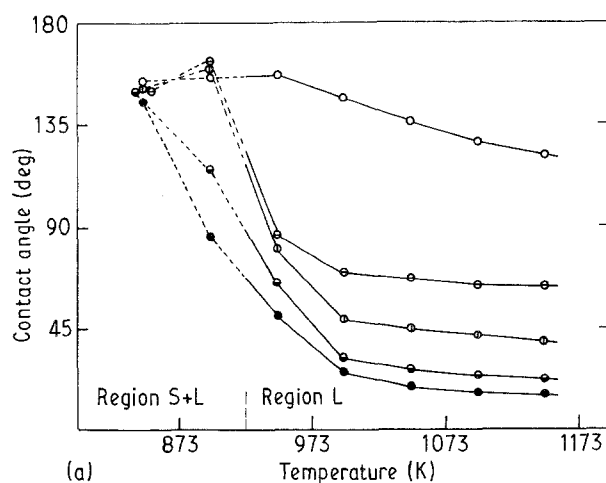
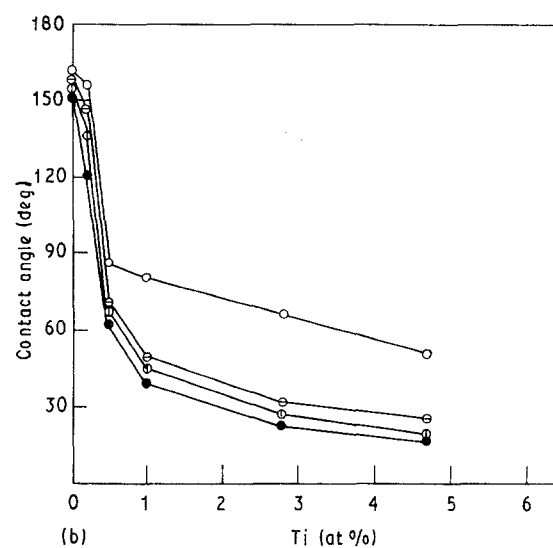


Figure 4 Dependence on temperature of the wettability of the sintered oxides by $\text{Ag}_{65}\text{In}_{35}$ alloy: (○) alumina, (●) zirconia.



(a)



(b)

Figure 5 (a) Dependence on temperature of the wettability by AgIn-Ti alloys of the sintered zirconia. Ti (at %): (○) 0.2, (⊖) 0.5, (⊕) 1.0, (⊙) 2.8, (●) 4.7. (b) Dependence of the contact angle between the alloy melts and the sintered zirconia on titanium content. T (K): (○) 950, (⊖) 1000, (⊕) 1050, (●) 1150.

ature. The contact angle of AgIn-0.2Ti/ZrO_2 decreased in the test-temperature range from 156° at 900 K to 121° at 1150 K. With increasing titanium addition, the wettability of the system became sensitive to temperature in the 900–950 K range. For example, at 0.5 at % Ti addition to the Ag-In base alloy, the wettability obviously increased with increasing temperature; the contact angle of the system was rapidly lowered from 163° at 900 K to 87° at 950 K.

Examination of Fig. 5a reveals two distinct stages in the variation of contact angle with temperature. Stage 1 is the melting stage. On melting, the temperature of the alloy samples was lower than 923 K under the liquidus temperature, and thus there existed some solid clusters in the molten samples. The activity of titanium in the alloy samples was lower, and the interfacial reaction between the molten alloy and ZrO_2 was weak at this stage. Hence, the contact angle of the AgIn-Ti/ZrO_2 system, other than the AgIn-4.7Ti alloy, was higher than 90° in the “no-wetting” state. In stage 2, the contact angle was rapidly reduced. By the end of this stage, the droplet equilib-

rated to a steady contact angle. From this figure it is clear that the contact angle of the system, except for the AgIn–0.2Ti alloy, is close to equilibrium over 1000 K.

Fig. 5b depicts the isotherms of the variation in contact angle with titanium content in the alloy. The contact angle of the system rapidly decreases with increasing titanium addition in the low titanium content region (< 1.0 at % Ti), and then the contact angle decreases slowly with titanium addition. On the 1000 K isotherm, on increasing the titanium content from 0 at % to 1.0 at %, the contact angle was lowered from 155° to about 50° , and with further rise in titanium content from 1.0 at % to 4.7 at % the contact angle was lowered from about 50° to 26° .

3.3. Wettability of the AgIn–Ti/Al₂O₃ system

The wetting of Al₂O₃ by the molten AgIn–Ti alloys is shown in Fig. 6a, which represents the variation in contact angle with temperature. From this figure it is obvious that a small titanium addition to the Ag–In

base alloy can more significantly improve the wetting of Al₂O₃ by the molten alloy and the contact angle of this system is more sensitive to temperature than is that of the AgIn–Ti/ZrO₂ system. The contact angle of the Al₂O₃ substrate with the alloy containing only 0.065 at % Ti in the 950–1150 K temperature range, is lowered from 143° to about 93° . Similar to that of AgIn–Ti/ZrO₂, the variation of the wetting with temperature of this system also exists at two stages, i.e. the melting stage and the rapidly reducing contact angle stage.

Fig. 6a also indicates that when the titanium content in the alloy is higher than 1.1 at %, the contact angle of this system decreases to less than 90° in the stage I temperature region, and a “no-wetting” transition takes place.

Fig. 6b depicts the isotherms of the variation of the contact angle with titanium content in the alloy. Similar to the AgIn–Ti/ZrO₂ system, the contact angle of the system rapidly falls with increasing titanium content in the region where Ti < 1.0 at %. At 1000 K isotherm, the contact angle is reduced from 150° at 0 at % Ti to about 27° at 1.1 at % Ti, and then when the titanium content is higher than 1.1 at %, the contact angle changes slowly and reaches a minimum value; thereafter the contact angle increases slowly with titanium addition. This tendency has also been observed in the molten Sn–Ti alloy/Al₂O₃ system [7].

From the above results, it is obvious that titanium is an intensive reactive element of the interface between the molten alloy and the oxides, and it can very significantly improve the wetting of the molten alloy on the oxides at mid-temperatures. However, a clear difference exists in the wettability of the AgIn–Ti alloy on the alumina substrate and the zirconia substrate. Comparing the test results for AgIn–Ti/Al₂O₃ with those of AgIn–Ti/ZrO₂, it is seen that the contact angle of the AgIn–Ti/Al₂O₃ system is lower than that of the AgIn–Ti/ZrO₂ system at the same temperature and titanium content, i.e. the wettability of the AgIn–Ti/Al₂O₃ system is better than that of the AgIn–Ti/ZrO₂ system under the same experimental conditions. This phenomenon is similar to that of the wetting of pure aluminium on both oxides [12, 14].

This may be caused mainly by the difference in the surface energy of both solid oxides and the interfacial energy between them and the molten alloy. The difference in the surface energy between Al₂O₃ and ZrO₂ has been discussed in Section 3.1. The difference in the interfacial energy between the solid oxides and the molten alloy can be expounded by a contact thermodynamic model between the solid and the liquid. According to Warren’s simple two atomic layer interface thermodynamic model [19], the interfacial energy of the solid–liquid is in direct ratio with the melting temperature of the solid. Because ZrO₂ possesses a higher melting point than Al₂O₃, the melting temperature of ZrO₂ is 2950 K and that of Al₂O₃ is 2290 K [20], the interfacial energy of AgIn–Ti/ZrO₂ is higher than that of AgIn–Ti/Al₂O₃, and thus the contact angle of the AgIn–Ti/ZrO₂ system is larger than that of the AgIn–Ti/Al₂O₃ system, in accordance with Yong’s equation.

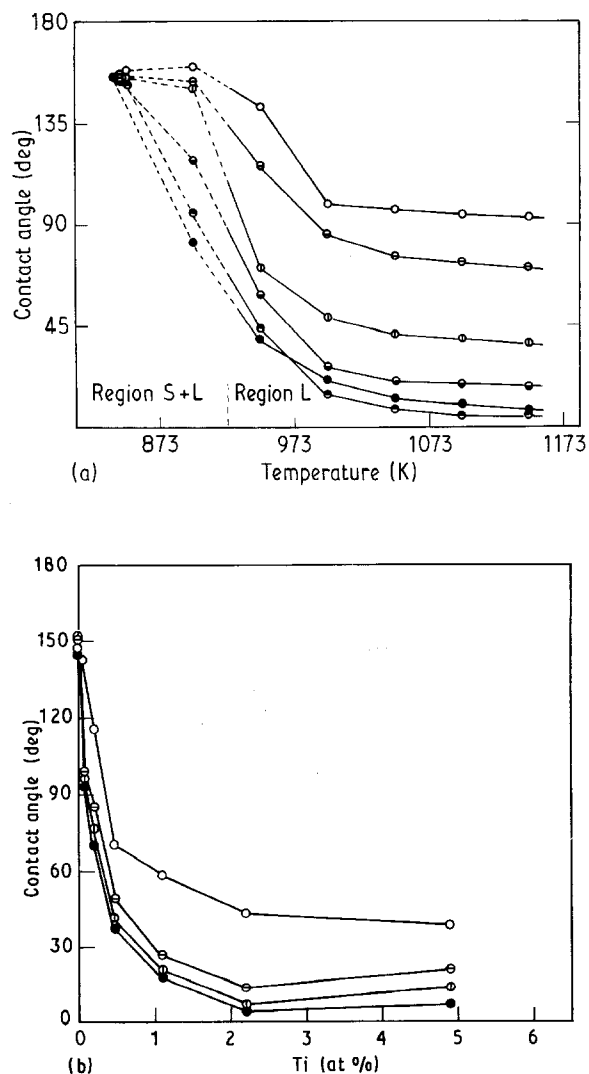


Figure 6 (a) Dependence on temperature of the wettability by AgIn–Ti alloys of the sintered alumina. Ti (at %): (○) 0.065, (⊖) 0.2, (⊕) 0.47, (●) 1.1, (⊙) 2.2, (●) 4.9. (b) Dependence of the contact angle between the alloy melts and the sintered alumina on titanium content. T (K): (○) 950, (⊖) 1000, (⊕) 1050, (●) 1150.

3.4. Interfacial reaction of the AgIn-Ti alloy with ZrO_2 and Al_2O_3

Some studies on the interaction phase formed between the alloy containing titanium and the oxides have been reported previously [1, 15, 21, 22], but some differences exist in their results. For instance, Naidich [1] reported that TiO formed in the contact zone between Cu-Ti alloy and Al_2O_3 , and Ti_2O_3 formed when Al_2O_3 was reacted with Sn-Ti alloy or Au-Ti alloy. Santella *et al.* [21] examined the ZrO_2 reaction with Ag-Cu-Ti alloy, and found that the reaction layer was TiO phase. Contrary to these results, after investigating the interaction layer of Ag-Cu-Ti/ Al_2O_3 , Pak *et al.* [22] indicated that the interaction layer consisted of Ti_2O , and Naka *et al.* [15] found that a series of Ti-O compounds, TiO_x , formed in the interfacial zone between Ag-Cu-Ti and alumina. From the previous studies, it can be considered that the various interaction phases formed depend on the experimental conditions.

In present work, the interfacial reaction zones of AgIn-3.7Ti/ Al_2O_3 and AgIn-4.0Ti/ ZrO_2 were examined using X-ray diffraction. The alloy samples also produced *in situ*, as in Fig. 1, were heated to 1173 K at

5 K min^{-1} , and held at that temperature for about 30 min. The weight of the sample was about 0.5 g. After the solidified droplet was mechanically separated from the oxide substrate, the surface of the reaction layer on the substrate was analysed by XRD.

Fig. 7 shows the X-ray diffraction pattern of the interfacial reaction layer between the AgIn-4.0Ti alloy and the ZrO_2 . From this figure it can be seen that the interfacial reaction phases consist of TiO and Ti_2O . The X-ray diffraction pattern of the reaction layer of the AgIn-3.7Ti alloy on Al_2O_3 is shown in Fig. 8. From Fig. 8 it is noted that the interfacial reaction phases are Ti_2O_2 , TiO, and Ti_2O . On comparison with previous works, the XRD results of the interaction layer of the AgIn-Ti alloy with the oxides are similar to those reported by Naka *et al.* [15]. However, the interfacial reaction phases of AgIn-Ti/ Al_2O_3 clearly differ from those of AgIn-Ti/ ZrO_2 .

This phenomenon may be attributed to the difference between the thermodynamic reaction in the alloy with alumina and in the alloy with zirconia. If it is considered that the reaction phases are only TiO and Ti_2O , for the Ti/ Al_2O_3 the chemical reaction is as

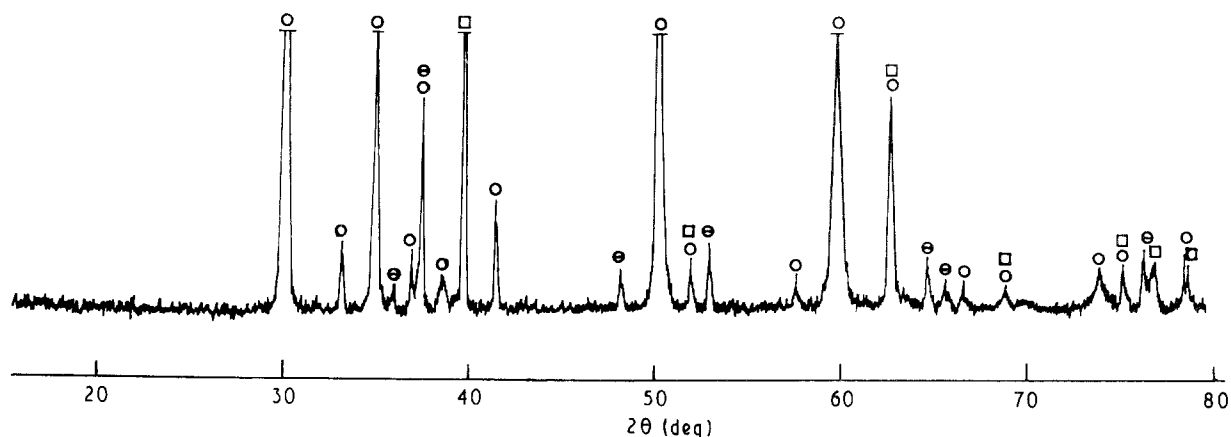


Figure 7 XRD pattern from CuK_{α} radiation for the interfacial reaction layer for AgIn-4.0Ti on the sintered zirconia. (o) Peaks belonging to the alloy sample and oxide substrate. The other peaks belong to the reaction layer: (□) Ti_2O (⊙) TiO.

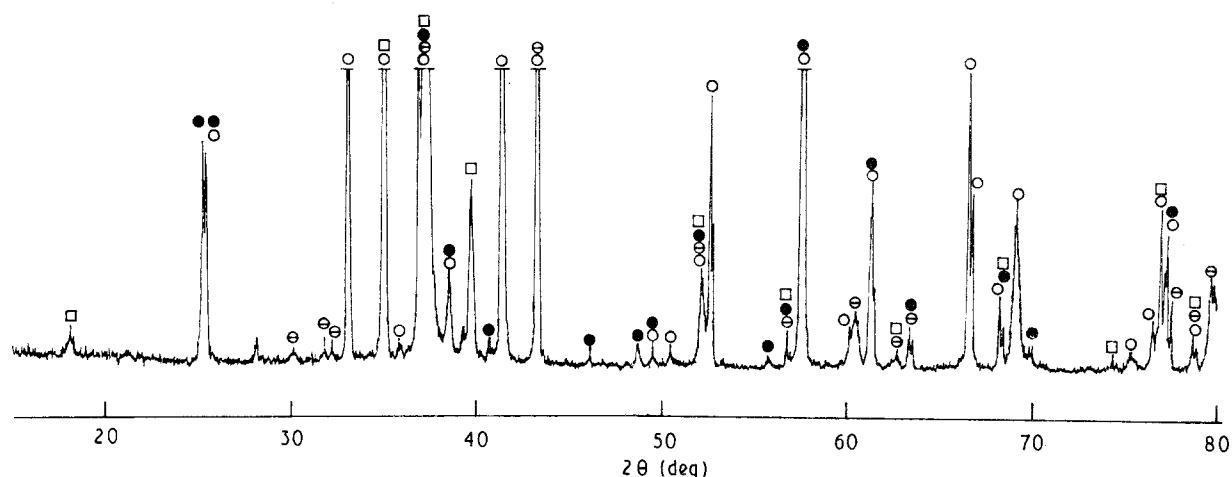
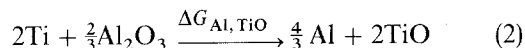
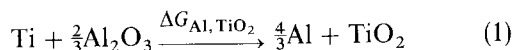
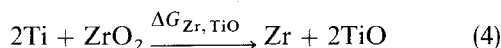
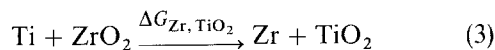


Figure 8 XRD pattern from CuK_{α} radiation for the interfacial reaction layer for AgIn-3.7Ti on the sintered alumina. (o) Peaks belonging to the alloy sample and oxide substrate. The other peaks belong to reaction layer: (□) Ti_2O , (⊙) TiO, (●) Ti_2O_2 .

follows



and for the Ti/ZrO₂



At 1173 K their free energy change can be calculated from the data given by Weast and Astle [20]: $\Delta G_{\text{Al, TiO}_2} = 32.4 \text{ kcal mol}^{-1}$, $\Delta G_{\text{Al, TiO}} = 12.6 \text{ kcal mol}^{-1}$, $\Delta G_{\text{Zr, TiO}_2} = 33.7 \text{ kcal mol}^{-1}$, $\Delta G_{\text{Zr, TiO}} = 13.8 \text{ kcal mol}^{-1}$. According to the free energy changes, the relation of the activity of titanium at interface with that of the product of the various reactions at equilibrium, aluminium and zirconium, can be calculated as follows:

for Reaction 1

$$a_{\text{Al}} = 2.97 \times 10^{-5} (a_{\text{Ti}})^{3/4} \quad (5)$$

for Reaction 2

$$a_{\text{Al}} = 1.73 \times 10^{-2} (a_{\text{Ti}})^{3/2} \quad (6)$$

for Reaction 3

$$a_{\text{Zr}} = 5.25 \times 10^{-7} a_{\text{Ti}} \quad (7)$$

for Reaction 4

$$a_{\text{Zr}} = 2.68 \times 10^{-3} (a_{\text{Ti}})^2 \quad (8)$$

The activity coefficient of titanium in Ag–Cu–3.1 at % Ti melt measured by Pak *et al.* is about 1.8 at 1000°C, and indium has no clear effect on it [22]. Hence, the estimated value of 0.1 of the activity of titanium in the molten Ag–In alloy containing about 4 at % Ti in the test, is reasonable. By substituting the estimated value of the activity of titanium into Equations 5–8, the activity of the reaction products aluminium and zirconium in Reactions 1–4, can be obtained. Comparing them with each other, and measuring the interaction phase, TiO₂ which formed in Reaction 3, is very difficult, because the activity of the zirconium product is very low.

On the other hand, zirconia possesses a higher melting point and larger chemical stability, so its dissociation rate in the molten AgIn–Ti alloy is lower than that of alumina. Hence it can hinder more effectively the penetration of titanium so that excessive titanium may exist in the interface. The excessive

titanium in the interface would result in the formation of low-valence Ti–O compound.

4. Conclusion

The effects of titanium addition on the wettability of alumina and zirconia by molten Ag–In alloy were measured using the sessile drop method at temperatures between 873 and 1150 K. The results show that small titanium additions can significantly improve the wetting of the Ag–In base alloy on alumina and zirconia. Furthermore, the contact angle in both systems indicates that the wettability of the AgIn–Ti/Al₂O₃ system is better than that of the alloy with the ZrO₂ system. X-ray diffraction analysis shows that the interaction phases of the alloy on alumina are TiO₂, TiO, and Ti₂O, and on zirconia are TiO and Ti₂O. This result was explained from the reaction thermodynamics viewpoint.

References

1. Ju. V. NAIDICH, *Prog. Surf. Membr. Sci.* **14** (1981) 353.
2. X. M. XUE, J. T. WANG and M. X. QUAN, *Mater. Sci. Engng A* **132** (1991) 277.
3. *Idem*, *J. Mater. Sci.*, **26** (1991) 6391
4. R. R. KAPOOR and T. W. ZAGAR, *Metall. Trans.* **20B** (1989) 919.
5. *Idem*, *Scripta Metall.* **22** (1988) 1277.
6. M. G. NICHOLAS, T. M. VALENTINE and M. J. WAITE, *J. Mater. Sci.* **15** (1980) 2197
7. M. YOKOTA, N. FUKUDA, H. NAGAI and K. SHOJI, *J. Jpn Inst. Metals* **53** (1989) 439.
8. M. UEKI, M. NAKA and I. OKAMOTO, *J. Mater. Sci.* **23** (1988) 2983.
9. R. M. CRISPIN and M. NICHOLAS, *J. Mater. Sci.* **11** (1976) 17.
10. J. G. DUH, W. S. CHIEN and B. S. CHIOU, *J. Mater. Sci. Lett.* **8** (1989) 405.
11. P. NIKOLOPOULOS and D. SOTIROPOULOU, *ibid.* **6** (1987) 1429.
12. M. UEKI, M. NAKA and I. OKAMOTO, *ibid.* **5** (1986) 1261.
13. M. NAKA, K. SAMPATH, I. OKAMOTO and Y. ARATA, *Trans. Jpn Weld. Res. Ins.* **12** [2] (1983) 181.
14. M. NAKA, K. SAMPATH, I. OKAMOTO, Y. ARATA, *Trans. Jap. Weld. Res. Inst.* **13** (2) (1984) 29.
15. *Idem*, *ibid.* **14** (1) (1985) 193.
16. J. T. WANG, M. S. BIAN and M. C. ZENG, *Acta Metall. Sinica* **17** (1981) 359.
17. M. S. BIAN, Q. CHEN and J. T. WANG, *ibid.* **24** (1988) B139.
18. D. T. LIVEY and P. MURRAY, *J. Amer. Ceram. Soc.* **39** (1956) 363.
19. R. WARREN, *J. Mater. Sci.* **15** (1980) 2489.
20. R. C. WEAST and M. J. ASTLE, "CRC Handbook of Chemistry and Physics", 63rd Edn. (CRC Press 1983).
21. M. L. SANTELLA, A. T. FISHER and C. P. HALTOM, *J. Electron Microsc. Tech.* **8** (1988) 211
22. J. J. PAK, M. L. SANTELLA and R. J. FRUEHAN, *Metall. Trans.* **21B** (1990) 349.

Received 27 November 1991

and accepted 25 June 1992